A. SPECIFIC AIMS:

A.1. Overview: The promise of improved MRI results at high field strength is compromised by the difficulties encountered at high field, including: i) Non-uniform excitation, due to the non-uniform B_1 field inherent at high field. Typically, the non-uniform excitation produces non-uniform tissue contrast, although other deleterious effects can be produced as well. ii) Large susceptibility gradients, which can distort slice positions unless large slice-select gradients are used. However, the limited RF power available on high field systems severely limits the gradient strength that can be used for T2-weighted images. The specific aims propose the further development and refinement of two new RF pulse designs to ameliorate these deleterious effects. **In addition, further development of software for simulating MRI experiments is proposed to aid in effective implementation of these new RF pulses into suitably re-designed MRI experiments.**

Specific aim 1: Pulses with immunity to B_1 inhomogeneity. The new B_1-insensitive design is based on optimized concatenations of rectangular pulses applied along different axes in the rotating frame, where the optimization is for both uniform tip and immunity to resonance offset. The design focuses on excitation pulses, but includes extension of the method to spin echo and inversion pulses.

Specific aim 2: Lowered peak voltage spin echo frequency-selective pulses. The new, lowered peak voltage design method consists of concatenation of conventional, frequency-selective pulses with gradients of alternating sign. The design includes spoiler gradients incorporated into the spin echo pulse to shorten the overall length of the pulse. Operation of these pulses in inhomogeneous B_1 fields is also considered.

Specific aim 3: Further development of MRI simulation software with inclusion of "inadvertent" magnetization transfer (MT) effects. The further development builds on software already developed for MP RAGE MRI experiments, and will include extended phase graph (EPG) algorithms to cover a wide range of MRI experiments. These simulations will aid in effective implementation of the new RF pulses, and avoid deleterious MT effects. A further use of these simulations is expected to be in the optimization of MRI sequences for 4.0 Tesla.

B. BACKGROUND AND SIGNIFICANCE

B.1. The Need for Pulses with Immunity to B_1 Imperfections: Even with a headcoil that produces a relatively homogeneous B_1 field, conductive and dielectric effects at high magnetic field distort the B_1 field and prevent uniform tipping, and also produce non-uniform reception of MR signals[1-3]. At 4.0 T, our experimental measurements have shown the non-uniformity in tipping to be approximately +/-20% to 25%, and the non-uniformity is considerably worse than this at still higher field strengths. While the non-uniform reception is potentially correctable[4-11], the spatially non-uniform excitation produces spatially non-uniform contrasts which is not correctable, making interpretation and clinical diagnosis more difficult. Even in cases in which the contrast is maintained over considerable variation in tip angle (as our simulations have shown for MPRAGE experiments), incorrect tip angles invariable lead to some kind of loss; for example, too shallow a tip leads to S/N loss, while too strong a tip does lead to loss in contrast. Finally, many relaxation measurements rely on accurate knowledge of the tip angle in order to obtain accurate relaxation values.

The non-uniform excitation can potentially be avoided by use of adiabatic pulses, or other pulse designs that have immunity to B_1 inhomogeneity. While a single example of an adiabatic excitation pulse suitable for multislice MRI experiments has been published[12], its length and gradient requirements render it useful only in special circumstances where high RF power and high gradient strength and performance are available. While a shorter version of this pulse

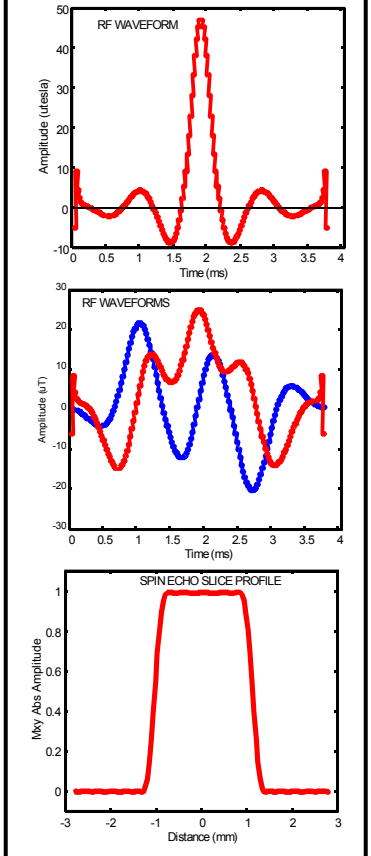

Fig. 1. Original spin echo pulse, root reflected form, and 2 mm slice profile.

exists, it exhibits excessive sensitivity to resonance offset and instrument settings[13] Thus, at present there does not exist a generally useful excitation pulse with immunity to B_1 inhomogeneity suitable for multislice MRI. While multidimensional pulses can in principle fill this void, they have disadvantages as well, including long duration and the need for a B_1 map prior to their design to combat the B_1 inhomogeneity. Although a recent report shows a relatively short (approximately 5 ms) slice-selective pulse with some compensation for B_1 inhomogeneity, this short duration was achieved by using a less-than-optimal gausssian profile[14]. In principle the long duration can be alleviated by implementation with RF SENSE methods; however, this approach requires specialized coils and multiple transmitters[15,16]. In addition, RF shimming methods, which also require multiple transmitters, have shown promise at very high field. Both of these latter two methodologies are very sophisticated and very expensive.

Slice-selective adiabatic inversion and spin echo pulses, such as the hyperbolic secant[17] and related pulses[18], are available. In addition, we note that a set of dual hyperbolic secant inversion pulses (but not concatenated) can function as a spin echo pulse with lower power deposition than a single, spin echo adiabatic pulse[18]. Thus, the need for additional inversion and spin echo pulses is not as severe as for excite pulses. There is, however, a price to be paid for use of adiabatic pulses: Unless the inversion pulse is made quite long (large μ), the transition zones of the selection profile are large. In addition, the total rotation (rotation an on-resonance spin would experience) is quite high, as is the power deposition for the pulse. Finally, these adiabatic pulses are typically functional over a very large range of B_1 inhomogeneity, in many cases ranging up to a factor of 10 or more. However, most MR experiments on human head require at most immunity to B_1 inhomogeneity of a factor of two. Even with surface coil measurements, the lessened signal strength in tissue regions beyond where the reduction of the B_1 field has been reduced by a factor of two usually renders the signal from this region of little value.

In summary, there remains an urgent need for useable excitation pulses with immunity to B_1 inhomogeneity of at least +/- 20 to 25%, which can be used for multislice MRI. Moreover, inversion and spin echo pulses with this same immunity to B_1 inhomogeneity but with less total rotation requirement than the hyperbolic secant pulse would represent very useful additions.

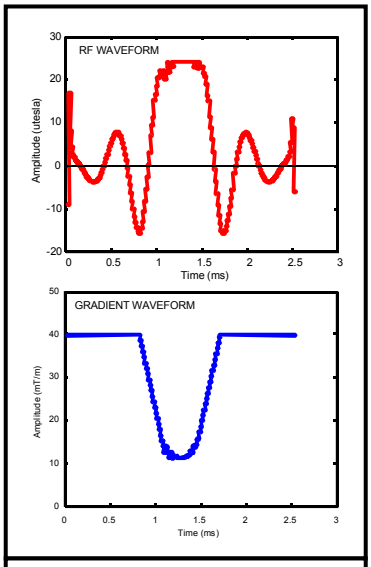

Fig. 2: Re-mapped spin echo pulse and associated gradient waveform.

B.2. The Need for Lowered Peak Voltage Pulses: One of the initial problems encountered with whole body MR systems at high field is the lack of B_1 field strength. Headcoils designed for 1.5 T conventionally produce maximum B_1 fields of from 50 to 70 μT. However, the combination of increased coil loading at high field, SAR concerns, and the price of high power RF amplifiers, typically limits B_1 field strengths of a headcoil loaded with the human head for MR systems at high field to from 20 to 25 μT. The lack of B_1 field strength limits the gradient strength that can be used for conventional pulses, and necessitates the use of long pulses (especially for spin echo pulses) applied with weaker gradients. However, susceptibility artifacts worsen at high field, and larger gradients are required to lessen slice distortions due to these artifacts. For example, if the sample frequency varies by 100 Hz, and the gradient produces only 100 Hz over the selected slice, the slice is mis-registered by the slice width where the frequency changes by 100 Hz. Even a gradient that produces 1 kHz over the slice has a mis-registration of up to 10%. Frequency variations of this order are not unreasonable for human head MRI at 4.0 Tesla[19-21], although some improvement can be obtained by use of an intra-oral passive shim[21,22], or proper head angulation[19]. Slice distortions can create difficulties in co-registration, and add to the difficulty of examination of morphological changes over time. In addition, the shortening of T_2* at high fields mandates the use of relatively short pulses, both to avoid signal losses, as well as to avoid degradation of the selection profile[23].

The need for lowered peak voltage pulses is particularly acute for 180 degree spin echo pulses, as the peak voltage of a spin echo pulse approximately 4 times that for a comparable 90 degree excitation pulse[23]. Typical methods to reduce the peak voltage on spin echo pulses include i) lowering the rotation angle, ii) using root reflection to lower the peak voltage, and iii) using VERSE[24] methods to lower peak voltage requirements. These methods do not alter the slice profile. However, lowering the rotation angle has the obvious

disadvantage of reducing the signal. Root reflection can be accomplished with MATPULSE (Fig. 1), but typically reduces the voltage by less than 50%. Finally, MATPULSE has its own version of VERSE, entitled remapping (Fig. 2). Remapping is more versatile than root reflection, and can even be used to shorten the pulse duration. However, excessive drooping of the gradient leads to excess sensitivity to resonance offset[23,24]. Thus, there remains an urgent need for spin echo pulses with lowered peak voltage requirements, particularly at high field.

B.3. Computer Simulation of MRI Sequences: Computer simulations of MRI experiments are playing an increasingly important role in the design and optimization MRI sequences, and can even be used to calculate tip angles to provide a prescribed signal level[25-27]. For example, simulations based on the extended phase graph (EPG) algorithm[28,29] have been used to show that programmed reductions in tips in Turbo Spin Echo (TSE) (also known as RARE or FSE) sequences can be optimized to retain a maximum signal, given the final tip angle[26,30]. In addition, similar simulations have been used to optimize a version of MP RAGE known as MP SAGE[27], and have also been used for demonstrating a RARE readout of a 2D MP RAGE experiment[31]. Some extension of these types of simulations would enable the effects of B_1 inhomogeneity to be examined, and potentially reduced, and also enable inadvertent magnetization transfer (MT) effects to be examined and avoided. In principle, EPG algorithms can include the effects of resonance offsets, although the PI is not aware of previous EPG calculations including resonance offset. Finally, simulations will provide important guidance for MRI sequence design at 4.0 Tesla to take maximum advantage of acceleration methods under development in other sections of this proposal.

C. Preliminary Results

C.1. Previous Studies by the Investigator of this Project: The PI, Dr. Matson, has a long-standing interest in shaped RF pulses, and has developed a comprehensive program in Matlab (MatPulse)[23] for generation of Shinnar - Le Roux (SLR) pulses, and for performing many other pulse manipulations including root reflection, gradient modulation as in the VERSE technique[32], and other manipulations including relaxation effects. His MatPulse program is available at **http://www.cind.research.va.gov/software/index.asp.** More recent activities include development of RF pulses with immunity to B_1 inhomogeneity for multislice MRI excitation[33], improved pulse designs for arterial spin labeling with matched magnetization transfer[34], and development of proton spectroscopic imaging at 7 Tesla for mouse brain studies with 1 mm resolution[35].

C.2. Pulses with immunity to B_1 inhomogeneity: Even with a headcoil that produces a relatively homogeneous B_1 field, dielectric effects at high magnetic field distort the B_1 field and prevent uniform tipping, and also produce non-uniform reception[1]. At 4 T, the non-uniformity in tipping with a headcoil is estimated to be +/- 20 to 25%, and the non-uniformity is considerably worse than this at still higher field strengths, or with other coil designs, such as surface coils, which produce non-uniform B_1 fields. The non-uniform excitation can be avoided by use of adiabatic pulses, or other pulse designs that have immunity to B_1 inhomogeneity. In the past, considerable effort has been expended to produce adiabatic pulses with immunities over a factor of 10. On the other hand, we[36] and others[37] have shown that the slice profile of adiabatic inversion pulses can be improved considerably by reducing the immunity of the pulse to B_1 inhomogeneity. However, with a single exception[12], adiabatic pulses suitable for multislice excitation no not exist (And the single exception is too long and energy intensive for general use). Even non-slice selective adiabatic excitation pulses, such as BIR4[38], are long and energy intensive. Thus, as discussed in the Background and Significance section, there remains an urgent need for a useable slice-selective excitation pulse with immunity to B_1 inhomogeneity which can be used for multislice MRI. In what we believe to represent new insights, we show here preliminary results which indicate that concatenated pulse designs can fulfill the role for uniform excitation with inhomogeneous B_1 fields, including slice selective pulses for multislice MRI. The general idea of concatenated, frequency selective pulses is not entirely new, as adiabatic spin echo[18] and excitation[12] pulses can be considered to be concatenated, frequency selective pulses, as may multi-dimensional pulses [39-46]. However, the catenation we present here involves pulses applied along different axes of the rotating frame, which is significantly different than the pulse designs mentioned above.

At the 1995 ENC Conference, the PI demonstrated that a symmetrical pulse with de-focusing and re-focusing gradients (Fig. 3) acts as does a rectangular pulse (pulse of constant amplitude applied along a single axis of the rotating field) in that it tips orthogonal magnetization, and preserves parallel magnetization. Thus, any concatenation of rectangular pulses can be replicated with this style of frequency selective pulse, although that does not necessarily mean that a useful pulse will be generated. Concatenation of two frequency selective pulses is depicted in Fig. 5. However, it should be noted that the pulses may be along different axes of the rotating frame. A more

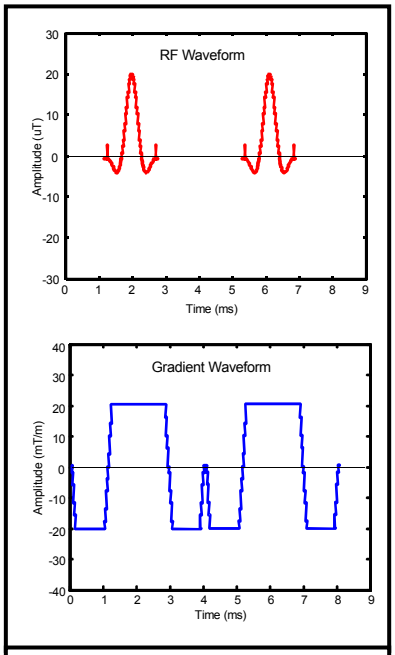

Fig. 3. RF pulse and gradient waveforms for concatenation.

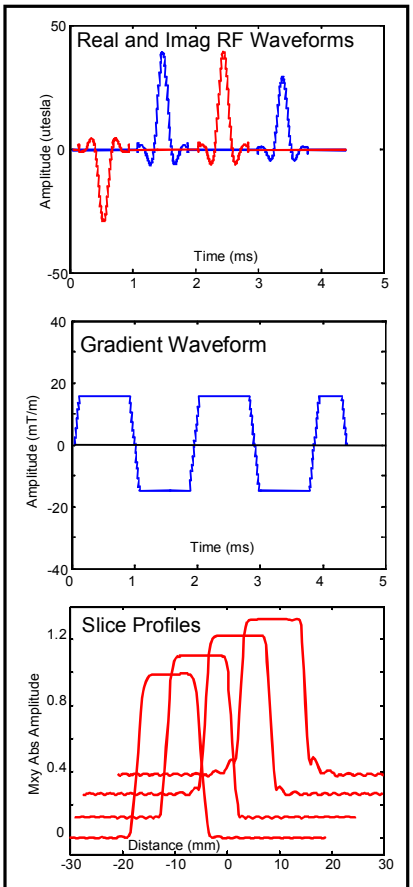

Fig. 4. RF and gradient waveforms, and resulting pulse profiles (over a B_1 range of a factor of 3) for the Levitt sequence.

efficient concatenation procedure would be to reverse the sign of the gradient on subsequent pulse sections to eliminate the gradient pulses between the pulse segments. In addition, the initial gradient can be eliminated in excitation pulses, and both initial and final gradients avoided in inversion pulses.

The PI has shown a simple four pulse excitation sequence with B_1 immunity approaching a factor of two[33] (Appendix A), based on a modification of a composite pulse sequence developed by Levitt[47]. A 10 mm version of this pulse, designed along the lines of Fig. 3, but with reversed gradients, uses nominal tips of 45º, 60º, 60º, and 45º applied successively along the –Y', X', Y', and X' axes in the rotating frame (Fig. 4). The resulting magnitude profiles over a B_1 range of a factor of two are shown in the figure. However, although the sequence exhibits good immunity to B_1 inhomogeneity, it is sensitive to resonance offset. In addition, the sequence provides coalescence of the magnetizations, which is not necessary for many MRI experiments.

There exist two additional reports of sequences with immunity to B_1 inhomogeneity[48,49] along the lines of that shown in Fig. 3, but based on different rectangular sequences. However, the PI's simulation of these sequences showed them to be even more sensitive to resonance offset than the Levitt sequence (results not shown).

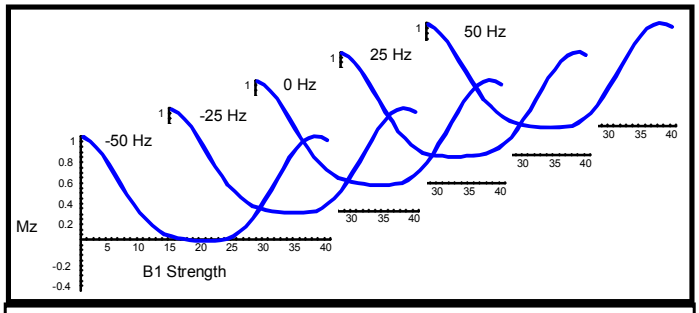

Fig. 5. Mz shown as a function of B_1 strength and resonance offsets from –50 Hz to 50 Hz for an optimized four pulse rectangular pulse 90^0 sequence.

Due to the limitations of the sequence based on the Levitt sequence, the PI developed computer optimization methods to seek out new three and four pulse rectangular composite pulse sequences that had immunity to both B_1 inhomogeneity and resonance offset. These sequences then form an improved basis for generation of slice selective pulses that confer both immunity to B_1 inhomogeneity and immunity to resonance offset to their slice selective counterparts. The optimization programs were developed in Mathematica (Wolfram Research), and made use of an application package from an independent developer (Global Optimization 4.2 by Loehle Enterprises). The optimization used the GlobalMinima program that utilizes an adaptive grid algorithm to find multiple solutions if they exist. A sample of the optimization program is included in Appendix B. Solutions have been obtained for tip angles from 15^0 to 90^0. These rectangular composite pulse sequences were then used as the basis for frequency selective pulses with immunity to both B_1 inhomogeneity and resonance offset[50] (Appendix C). Despite being longer, the four pulse sequences provided improved immunity to resonance offset.

Figure 5 shows the results of optimization of a four pulse rectangular pulse sequence in which the Mz magnetization is plotted as a function of B_1 strength for resonance offsets from –50 Hz to 50 Hz. A trace diagram showing the trajectories of unit magnetization vectors over the unit circle is shown in Fig. 6, where the position for the B_1 field of the final tip is shown. This figure demonstrates that, although the magnetizations are not coalesced, they are accurately tipped into the transverse plane.

The conversion to a 4 mm slice selective pulse is shown in Fig. 7, and the resulting profiles over a B_1 range of +/- 20% are shown in Fig. 8. This figure also shows that the sequence performs well over a resonance offset range of +/- 50 Hz, which is nearly double that of an equivalent sequence based on the Levitt sequence. While real and imaginary profiles are generally required to fully assess the performance of the sequence, in this case the real profile closely follows the magnitude profile.

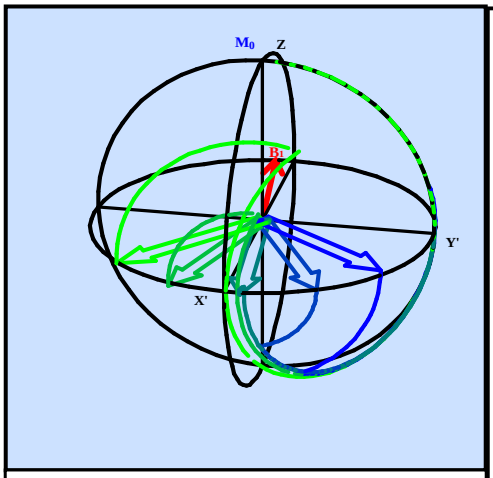

Fig. 6. Trace diagram for the four rectangular pulse 90^0 sequence

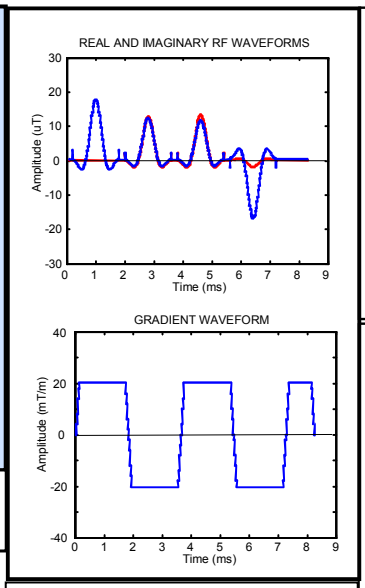

Fig. 7. RF and gradient waveforms for the 90^0 pulse.

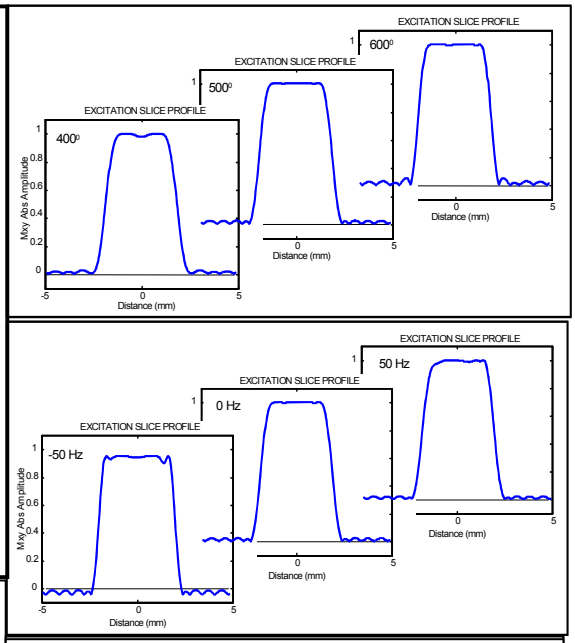

Fig. 8. Magnitude profiles over a B1 range of +/- 20%, and over a resonance offset range of +/- 50 Hz for the 90^0 pulse.

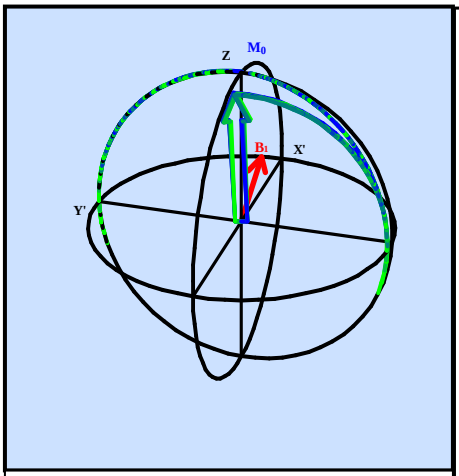

Fig. 9. Trace diagram for the rectangular pulse 15 degree sequence.

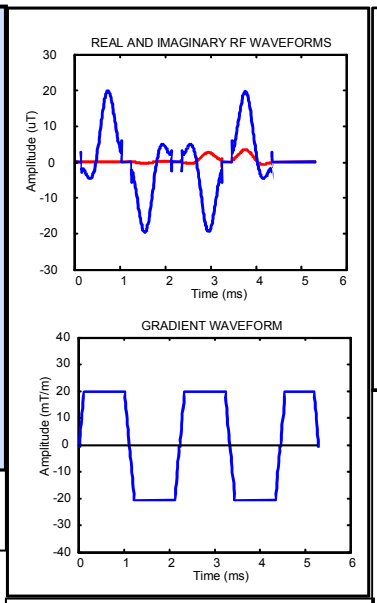

Fig.10. RF and gradient waveforms for the 15 degree sequence

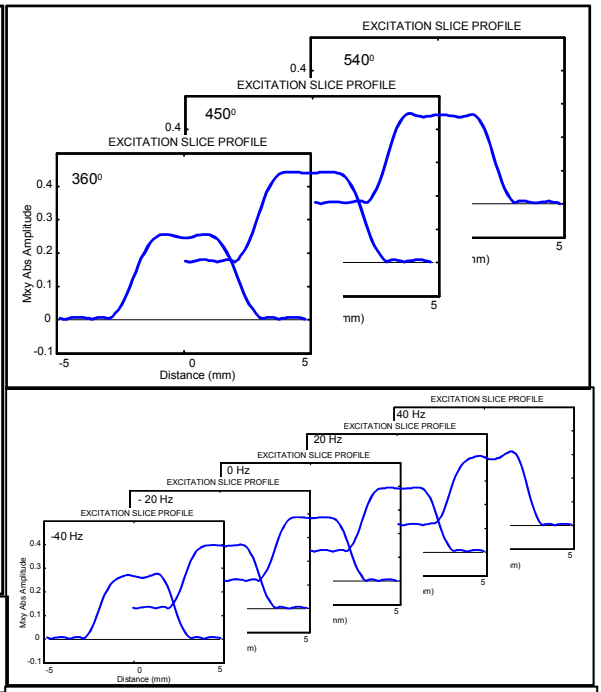

Fig. 11. Magnitude profiles over a B1 range of +/- 20%, and over a resonance offset range of +/- 40 Hz for the 15 degree sequence.

An example of the trace diagram of a shallow tip pulse (15^0) is shown in Fig. 9. Although the optimization program did not specify coalescence of the magnetizations, in this case the coalescence occurred naturally. Note that due to the coalescence the TE interval starts from the end of the pulse instead of from its middle, thus diminishing the disadvantage of the long pulse length. The 4 mm frequency selective version is shown in Fig. 10, and the resulting profiles over a B_1 range of +/- 20%, and over a resonance offset range of +/- 40 Hz, are shown in Fig. 11. Although the PI has shown that the Levitt sequence can be re-formulated to produce a

shallow tip pulse, that version is extremely sensitivity to resonance offset. The new sequence shown here is much more robust with respect to resonance offset than the levitt shallow tip sequence. However, for this shallow tip pulse the real and imaginary profiles are not as well behaved as in the 90^0 case, and additional signal loss (from 10 to 20%) over that indicated by the magnitude profile occurs. Finally, it is noted that since the 3D MPRAGE sequence does not use frequency selective excitation pulses, the composite rectangular pulse sequence can be used directly for the excitation pulse in the 3D MPRAGE experiment.

In summary, new rectangular pulse sequences have been developed by the PI to form the basis for frequency selective pulses with immunity to both B_1 inhomogeneity and to resonance offset. Preliminary designs shown here demonstrate useable sequences for both shallow and 90^0 tips for 4 mm slice thickness in human brain at 4.0 Tesla. However, the preliminary designs for pulses with immunity to B_1 inhomogeneity are not the final results, but will be subjected to additional optimization to generate the final designs. Furthermore, additional promising sequences uncovered by the optimization process have not yet been tested as slice selective pulses. In addition, we were not as successful in developing intermediate tip angle pulses, and will need to extend the number of pulses to 5 or 6 to better cover the possible range of pulses. Finally, the 4 mm slab thickness can be reduced to 2 mm slices through the larger gradients (40 mT/m available on the new Bruker MedSpec 4.0 Tesla instrument).

The chief drawback of these cascades is that they generate much higher SAR than the single selective pulse they replace. In addition, they provide uniform tipping over a limited range of B_1 inhomogeneity and resonance offset. Thus, **following our development of the above pulses,** our goal became to design pulse cascades of lower SAR, and with an extended range of performance.

C.3. Off-Resonance Pulses with immunity to B_1 inhomogeneity and Lowered SAR: We hypothesized that the use of off-resonance as a design parameter could provide additional flexibility for design of pulse cascades with immunity to both B_1 inhomogeneity and to spin resonance offset. An additional attraction for this design method was that the off-resonance component of the tipping field would not contribute to SAR. Accordingly, the Mathematica program described in [50] for optimization of rectangular pulse cascades was modified to incorporate off-resonance into the optimization.

Our optimization results incorporating off-resonance did produce lowered SAR rectangular pulse cascades, and also produced cascades with extended ranges of performance. However, the SLR pulse shapes generated with MatPulse[23] and used to convert from rectangular to slice-selective pulses produced markedly distorted profiles when used with the off-resonance pulses. To overcome this problem, each off-resonance pulse was converted into two identical frequency-selective shapes, applied with gradients of opposite signs. This approach produced acceptable slice-selective profiles provided the off-resonance pulses were limited in both rotation angle and degree of off-resonance. As an example of this approach, Fig. 12 shows the magnitude profile for a 60 degree off-resonance frequency-selective pulse, while Fig. 13 shows the improvement by conversion of the pulse into two 30 degree off-resonance pulses applied in the presence of alternating sign gradients.

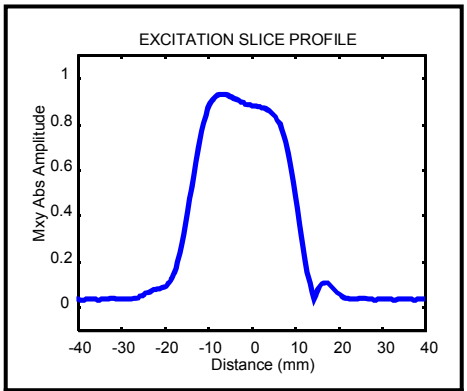

Fig. 12. Magnitude profile for a single 60 degree frequency-selective off-resonance pulse.

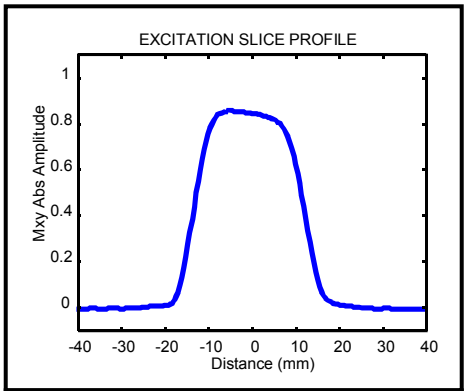

Fig. 13. Magnitude profile for two cascaded 30 degree frequency-selective off-resonance pulses.

As an example of generation of a 90 degree pulse, Fig. 14 shows the longitudinal magnetization for a three pulse rectangular sequence producing a 90 degree tip as a function of B_1 strength (arbitrary units). The sequence utilizes an on-resonance pulse of 45 degrees, followed by an off-resonance pulse of 120 degrees, and a final on-resonance pulse of 70 degrees. Figure 14 shows that the sequence produces close to a 90 degree pulse (90 +/- 5 degrees) over a B_1 range of a factor of two, and over a resonance offset of +/- 50 Hz. A trace diagram for magnetizations experiencing different B_1 strengths is shown in Fig. 15, where the middle pulse is the off-resonance pulse, and the direction of the B_1 field for the final tip is shown in red.

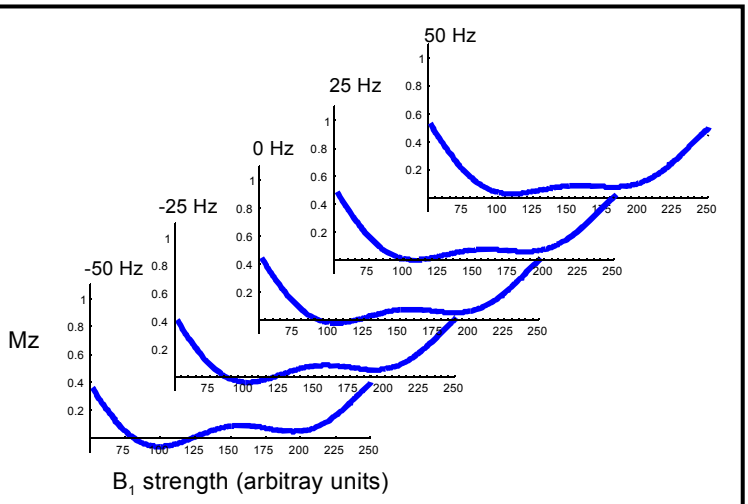

Fig. 14. Mz as a function of B_1 strength and resonance offset for the three-tip 90 degree pulse, with the central pulse designed with a resonance offset.

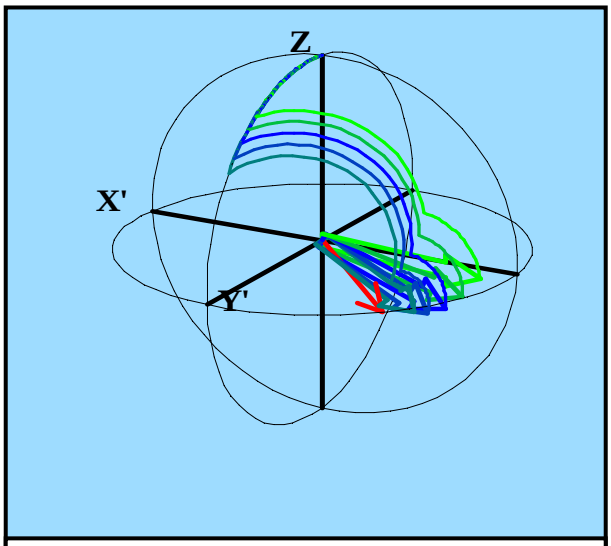

Fig. 15. Trace diagram of magnetizations experiencing different B_1 strengths for the 90 degree pulse using resonance offset.

Figure 16 shows the RF and gradient waveforms following conversion to a slice-selective cascade, where the middle 120 degree off-resonance pulse has been converted into two 60 degree off-resonance pulses. Figure 17 shows magnitude profiles of the slice selective cascade over a B_1 range of a factor of two, and profiles for resonance offsets of +/- 50 Hz. This cascade provides an extended B_1 range and similar resonance offset performance to the previously developed four pulse slice-selective cascade (Fig. 11). However, the previously developed sequence used four nominal 90 degree tips, while the off-resonance design used nominal tips of 45, 60, 60, and 70 degrees, thus producing approximately half of the SAR generated by the on-resonance design.

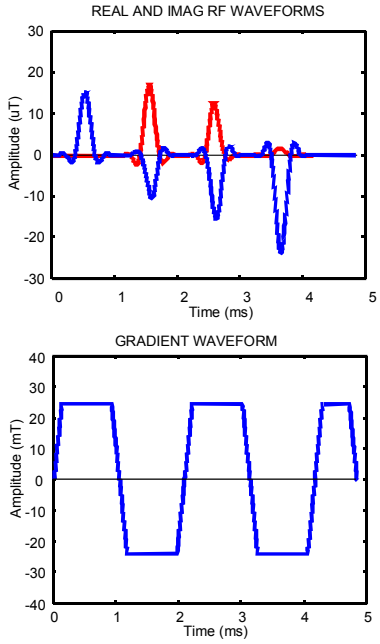

Fig. 16. RF and gradient waveforms for the 90 degree selective pulse utilizing off-resonance segments.

Finally, unlike the on-resonance selective pulse, the off-resonance selective pulse refocuses the resonance offsets so that the TE time starts at the end of the RF pulse, rather than at the middle of the pulse (as in conventional pulses). Thus, the length of the pulse does not necessarily determine the minimum TE time able to be used with this pulse. The effect of the refocusing is demonstrated in Fig. 18, which shows that, unlike conventional pulses, the phase of the magnetization does not change with resonance offset.

In summary, we have used off-resonance as a design parameter to generate new rectangular pulse cascades composed of both on-resonance and off-resonance segments to generate uniform tips in the presence of inhomogeneous B_1 fields and spin resonance offsets. In this preliminary investigation the conversion into slice-selective versions required limiting both the rotation angle and degree of off-resonance for the off-resonance segment of the pulses. Although this presentation only shows 90 degree selective pulses, we have also been able to produce shallow tip angle pulses utilizing off-resonance segments. We are in the process of developing optimization routines to see if optimization of the entire selective pulse cascade can be used to improve the utilization of off-resonance as a design parameter to provide uniform tipping in the presence of non-uniform B_1 fields.

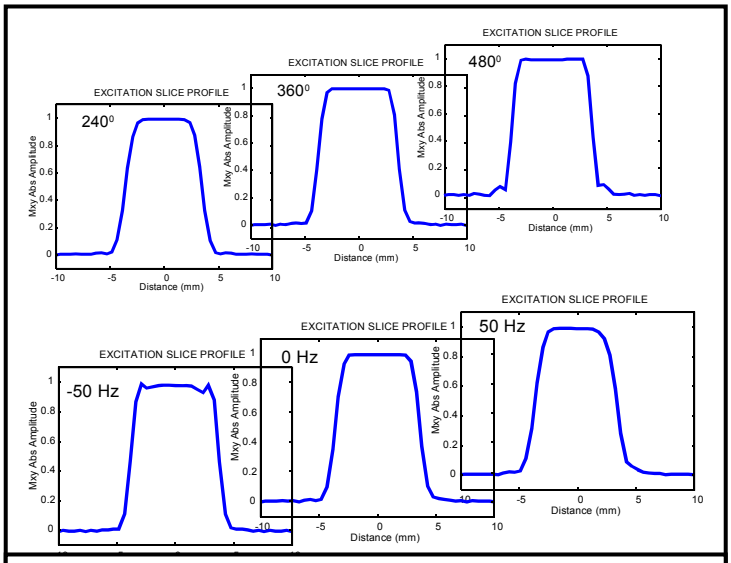

Fig. 17. Magnitude profiles for the 90 degree pulse of Fig. 9 over a B_1 inhomogeneity of a factor of two (upper profiles), and for resonance offsets over +/- 50 Hz (lower profiles).

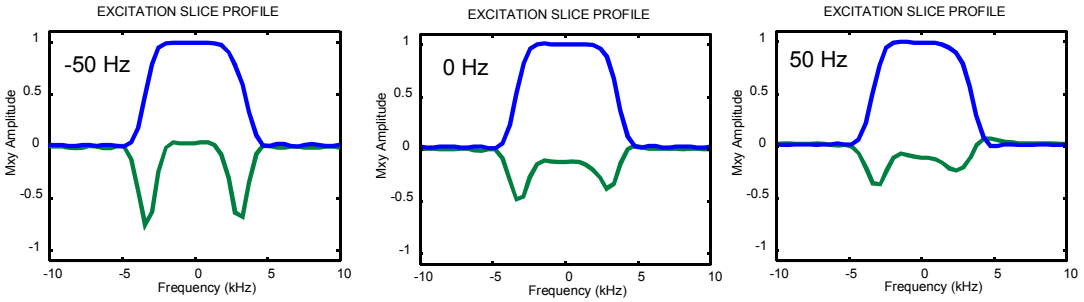

Fig. 18. Mx (green) and My (blue) magnetizations produced by the same refocusing gradient for resonance offsets from -50 Hz to +50 Hz. The figure shows the phase is unchanged over this range of resonance offsets.

C.4. Lowered Peak Voltage Pulses: In what we believe to represent new insights, we show here preliminary results which indicate that the restrictions resulting from limited B_1 strength can be ameliorated through the use of concatenated, frequency selective pulses designed for low peak voltage. However, the intent and design considerations for these previously designed pulses differs from the lowered peak voltage designs to be demonstrated in this proposal. Very recent examples of the types of concatenated, frequency- selective pulses to be demonstrated in this proposal do exist[51,52], including pulses demonstrated by the PI and Dr. Schleich[34] (Appendix D), although in these latter examples the concatenation was to enable time-reversed versions of the inversion pulses to be produced, and the lowered voltage was not a design consideration. In addition, as noted above another concatenated, frequency selective four pulse sequence with immunity to B_1 inhomogeneity has been presented by the PI[33] (Appendix A), and a version of this pulse has also been presented at the 2001 ENC conference. However, this latter pulse was designed for immunity to to B_1 (See below), and again, lowered peak voltage was not a consideration. Finally, if we imagine that crusher gradients equal to but opposite in sign to the initial and final gradients are applied, the sequence without the initial and final gradients acts as a crushed spin echo pulse, without the physical existence of crusher gradients. As far as

the PI can tell, this idea of frequency pulse concatenation with reversed gradients to generate a lowered peak voltage pulse represents a new design concept not previously published in the literature.

We now demonstrate a preliminary pulse design for a system with 20 mT/m gradients with a slew rate of 200 mT/m/ms, but with B_1 strength limited to under 25 μT. For comparison purposes, a 90º pulse (parent pulse) executed in a gradient of 20 mT/m to produce a nomimal 10 mm slice is shown in Fig. 19. This pulse has a high quality factor (time-bandwidth product of 16), resulting in an excellent slice profile (Fig. 19). A preliminary, concatenated pair of SLR 45º pulses and the resulting slice profile essentially equivalent to the parent pulse is shown in Fig. 20. As expected, the peak voltage is reduced by a factor of two. What is unexpected is that the concatenated pulse is barely longer than the parent pulse. The reason for this is somewhat complicated, but can be broken down into three effects. First, the concatenation process slightly narrows the excitation profile, so the pulses to be concatenated are designed for slightly greater bandwidth, which enables them to be slightly shorter, while still preserving the same quality (time bandwidth product). Second, the concatenation also slightly sharpens the excitation profile, so the concatenated pulses can be designed for slightly lower quality (larger transition zones) by shortening the pulse lengths still more. Thus, these two effects enable each concatenated pulse to be somewhat shorter than the parent pulse, while still accomplishing the equivalent overall excitation profile. Finally, because the individual pulses are shortened, the gradient required for refocusing is shortened as well. For comparison purposes, it should be realized that the parent pulse could still be executed to produce the same slice profile if the gradient were reduced by half, in which case the parent pulse amplitude would also be reduced by half, and the pulse duration doubled. However, in this case the concatenated version would be the pulse of shorter overall duration. In summary, the concept of concatenation of frequency selective pulses with reversed gradients to generate an equivalent pulse of lowered peak voltage and only slightly increased length represents a new concept in pulse design.

Although the concept of concatenating frequency selective pulses for lowered voltage has been demonstrated here for a 90 degree excitation pulse, the real need for lowered voltage pulses resides with spin echo (SE) pulses. A SLR SE pulse requires approximately 4 times the peak voltage of a corresponding 90 degree pulse). As an illustrative example, we consider a 3.2 kHz SLR SE pulse executed in the presence of a 20 mT/m gradient to produce a nominal 4 mm slice. Such a pulse requires a peak B_1 in excess of 70 uT Of course, our hypothetical MRI system, capable of a B_1 strength of only 25 uT, cannot produce this pulse. Fig. 21A shows a concatenation of three 60 degree pulses, which the system can produce. The crusher gradients, not shown in 21A, are added in 21B so as to just cancel the defocusing and re-focusing gradient lobes. The resulting pulse and gradient waveforms are displayed in Fig. 21C. Because the crusher gradients are now incorporated into the SE pulse itself, the concatenated length is barely longer than the original, high voltage crushed spin echo pulse (including crusher gradients). The voltage is much reduced, the SAR is reduced, and because the crusher gradients have been incorporated into the pulse, it appears that there is only a small price of slightly increased pulse duration to pay for the reductions in voltage and SAR! While in addition to SE (which can also perform as inversion) pulses, concatenation designs of excite and saturation pulses are straightforward, we believe that it is in the application of reduced voltage spin echo pulses that the concatenation design methods will have their most important role.

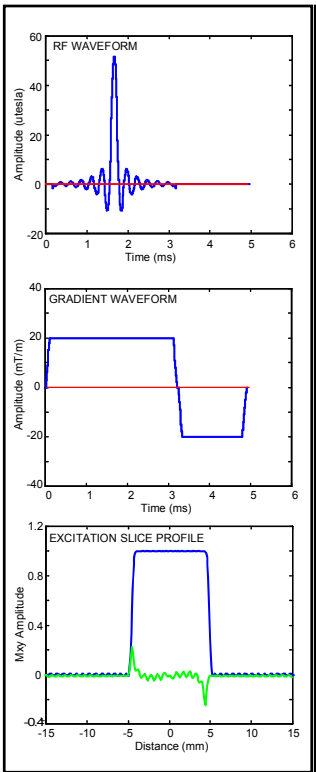

Fig.19. Parent 90 RF and gradient waveforms with slice profile.

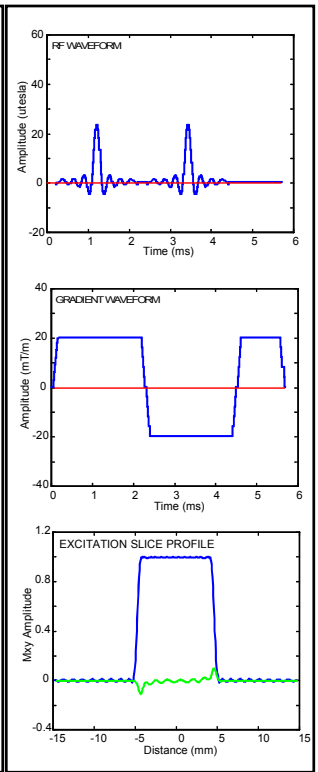

Fig. 20. Concatenated RF and gradient waveforms with slice profile.

A drawback of gradient reversed pulses is their sensitivity to resonance offset. Our own 4.0 Tesla measurements on human head indicate that the vast majority of the brain parenchyma can be shimmed to +/- 40 or 50 Hz, and these results are in agreement with a number of literature articles[19-21]. There are small regions around the sinuses (the inferior frontal cortex), and in the outer sections of the temporal lobe, and possibly the brainstem, in which the resonance offsets exceed these numbers, even when special means such as use of an intra-oral diamagnetic passive shim [21,22] or head angulation[19] is used to improve B_0 homogeneity. However, even conventional imaging methods typically produce distortions in these regions, and we believe pulses with immunity to resonance offsets of +/- 40 to 50 Hz can be considered as useful, as they produce reliable results over the vast majority of the brain parenchyma.

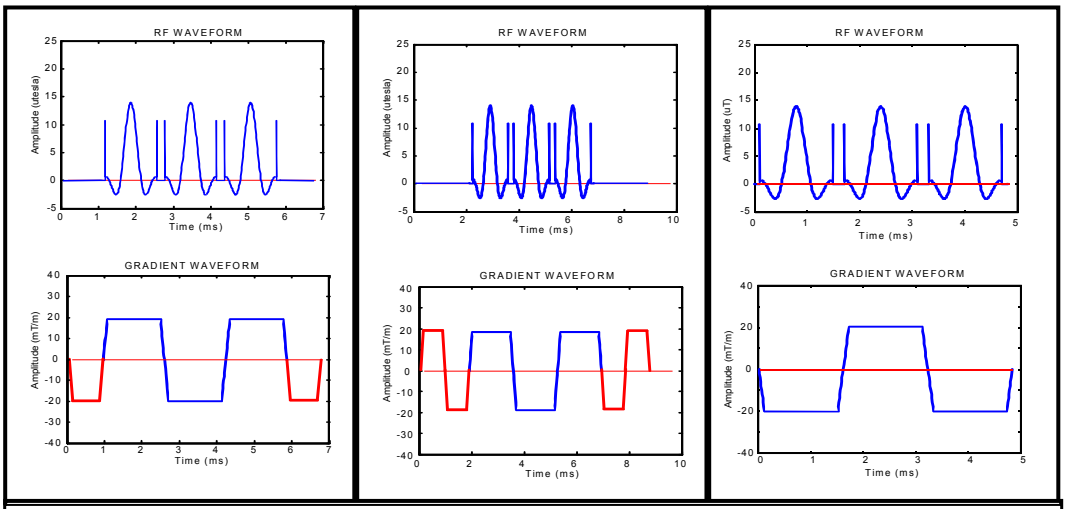

Fig. 21. (A) Concatenated SE pulse. (B) SE pulse with crusher gradients added. (C) Effective SE pulse with crusher gradients incorporated.

Figure 22 shows a series of "crushed profiles" generated by the pulse of Fig. 14C for resonance offsets from -50 Hz to +50 Hz. As shown, there is a signal loss approaching 20% for resonance offsets of 50 Hz, although there is no spatial shift of the profile with resonance offset (Results not shown). Note that the MatPulse "crushed profile" suppresses the high frequency spatial oscillations according to the prescription given by Pauley et al.[53]. Reducing the overall duration of the pulse diminishes its sensitivity to resonance offset. If more gradient and RF strengths are available, the shortening can be done by increasing both, while if only more gradient strength is available, the shortening can be done by re-mapping (See Background and Significance). If neither is available, the pulse can still be shortened, albeit at the expense of the quality of the excitation profile. Another approach to reducing the sensitivity to resonance offset is to utilize the pulse in a CPMG configuration, so that the phase is reversed on every other pulse, and only every second echo is collected. The resulting profile for 50 Hz resonance offset is shown in Fig. 23A, while Fig. 23B shows the result for both reduction of B_1 by 20%, and resonance offset of 50 Hz. These results show the CPMG phase cycling is reasonably effective for suppressing both sensitivity to resonance offset and non-uniform tipping due to B_1 inhomogeneity.

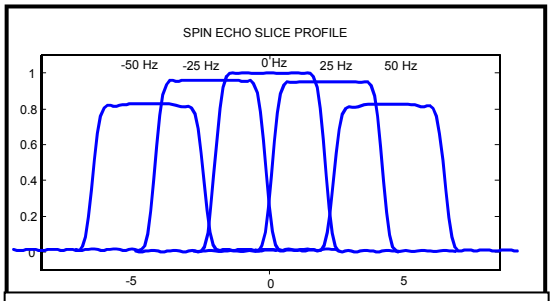

Fig. 22. Magnitude profiles for the SE pulse of Fig. 8, spanning the range of resonance offsets from –50 Hz to 50 Hz.

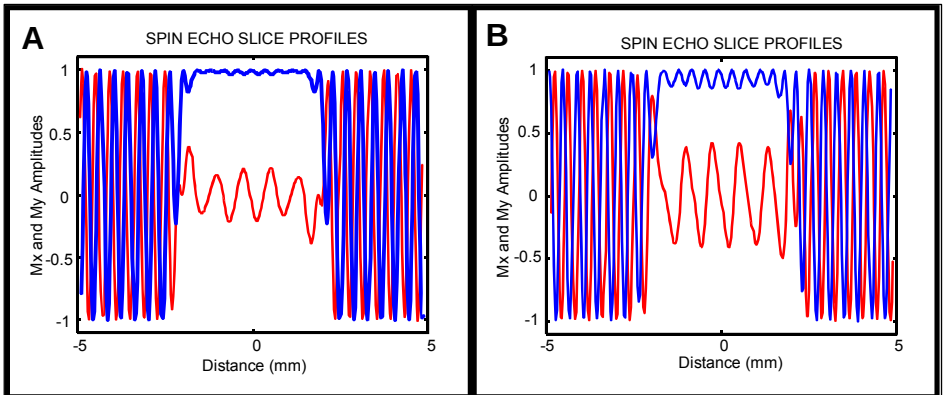

Fig. 23. Profiles of the second echo for the pulse of Fig. 8C in a CPMG sequence. (A) 50 Hz resonance offset. (B) 50 Hz resonance offset and B_1 reduced by 20%.

C.5. Evaluation of Magnetization Transfer Effects: **The total rotation (rotation an on-resonance spin would experience) of the B_1 insensitive pulses is much higher than that of the pulses they replace. For the non-selective pulses, the shallow tip B_1 insensitive pulse of Fig. 9 produced 360 degrees of total rotation, while for a 10 degree tip, a conventional, rectangular pulse produces only 10 degrees of total rotation. Although the total rotation of the shallow tip pulse can be reduced, the reduced tip may still be in the range of 180 degrees. A similar discrepancy exists for the slice-selective pulses as well. For example, a conventional 90 degree selective pulse might produce 120 to 150 degrees of total rotation, but both the shallow tip and 90 degree tip B_1 insensitive pulses shown above produce in the neighborhood of 200 to 400 degrees of total rotation (the exact amount depends on the design parameters). Thus, the B_1 insensitive pulses may produce unwanted MT effects. In order to assess the MT effects, the PI has begun developing a program (MatMRI) in Matlab using the GUI-capabilities of that program to calculate the MT effects for standard MRI sequences. At this point, only 2D MPRAGE and 3D MPRAGE experiments are completed, but implementation of a number of additional MRI experiments is planned. The PI is not aware of other calculations of this type, which include MT effects, and in the future will include sensitivity to resonance offsets, in the literature. The MatMRI program is available at: http://www.cind.research.va.gov/software/index.asp**

The MatMRI program makes use of the evolution and transfer equations for the saturation ($1-Mz/M^0z$) for a single component developed by Helms and Hagberg[54] for a two pool system. To be able to assess the MT effects separate from relaxation effects, calculations are also available for calculation of signal amplitudes with the MT effects excluded. These latter calculations follow along the lines suggested by Deichmann et al.[55]. At this juncture, the program only makes use of a single lineshape for the broad component (super-Lorentzian[56]), but the implementation of additional lineshapes is also planned. Recent results suggest that, except for the relaxation times, the tissue parameters for MT do not change significantly over the range of 1.5 to 3 Tesla[57], and are thus relatively field independent. In addition, recent literature values for MT parameters appear to be in general agreement[57-59]. Finally, MatMRI menus for the MPRAGE 2D and 3D calculations are provided as Appendix E, and an outline of the calculations for the MT effect is provided in Appendix F.

For the 3D MPRAGE experiment, all RF pulses act on all of the tissue, so MT effects were expected to be large for use of the B_1 insensitive pulses. Figure 24 shows the expected signal amplitudes without considering MT effects for gray matter, white matter, and CSF for the conventional 3D MPRAGE experiment using parameters presently in use at the CIND laboratory (adiabatic inversion, and 8 degree excitation tip, with additional parameters indicated in the figure). The vertical line indicates the time at which the center of k-space is acquired. Figure 25 shows the results when MT effects are included, which shows rather small changes to the white matter and gray matter. Figure 26 shows the same results when B_1 insensitive excitation pulses of 180 degrees of total rotation are used. The resulting reductions to the white and gray matter are dramatic, and clearly the use of the B_1 insensitive pulses for the 3D MPRAGE experiment on brain tissue is inadvisable. A preliminary viewing of some of these results was provided at the 2007 RR Site Visit.

The 3D MPRAGE represents a 'worst case" example, and MT effects are not expected to be as severe for the 2D MPRAGE experiment. While conventional thinking is that 3D experiments are more efficient than 2D experiments, is has also been argued that the sensitivities of 2D and 3D experiments are highly similar in a large number of practical situations[60]. Figure 27 shows a conventional 2D MPRAGE experiment, where parameters are similar to those in the 3D MPRAGE experiment, except a 30 degree excitation tip is assumed, and MT effects are ignored. Additional experimental parameters include excitation pulse bandwidths of 3.4 kHz, and intervals of 25 ms between inversion (or acquisition) of adjacent slices. Figure 28 includes MT effects, and shows that MT effects occur primarily due to the inversion pulses, and that the signal amplitudes during acquisition are actually slightly enhanced. The diminished Mz signal just prior to inversion is due to inversion pulses applied to neighboring slices. Figure 29 shows the same experiment executed with B_1 insensitive pulses. Although MT effects are now visible due to both inversion and excitation pulses, the reduction in Mz just prior to acquisition is small (on the order of 10 to 15%). This small reduction is signal amplitude is part of the price to pay to obtain uniform tipping over the entire brain.

Besides the larger total rotation produced by the B_1 insensitive pulses, they also produce increased SAR. One way to lower the SAR of the experiment is to lengthen the repetition time (TR). In addition, if signal can be increased, and array coil reception is being used, it may be possible to retain the original experiment (run) time by using a higher acceleration factor. In principle, the loss in S/N incurred by acceleration factors scales with the square root of the experiment time, so in principle if one can improve S/N by the square root of the increased TR, SAR is reduced but no other disadvantage is incurred. In reality, artifacts are incurred by the use of high acceleration factors, but improvements in suppression of such artifacts is a rapidly evolving field, with new approaches being pursued by other CIND scientists.

As a cursory example of this concept, Fig. 30 shows the previous 2D MPRAGE experiment (still implemented with B_1 insensitive pulses) implemented with longer TI and TR times. The figure illustrates that lengthening of the TR time from 2400 to 3000 ms provides a rather dramatic increase of S/N. Further discussion of this concept to lengthen TR to minimize SAR yet not incur a penalty in run time is provided in the Research Plan.

Finally, further development of MRI simulations are underway using extended phase graph (EPG) algorithms[28,29] and to be able to simulate a wide variety of MRI experiments.

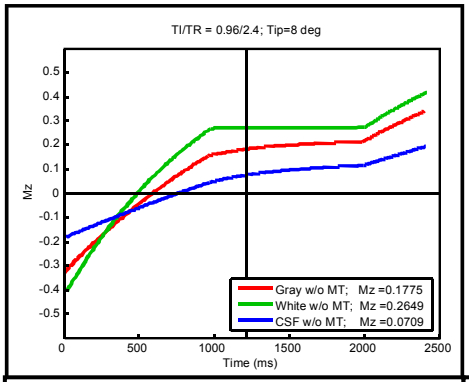

Fig. 24. 3D MPRAGE without magnetization transfer.

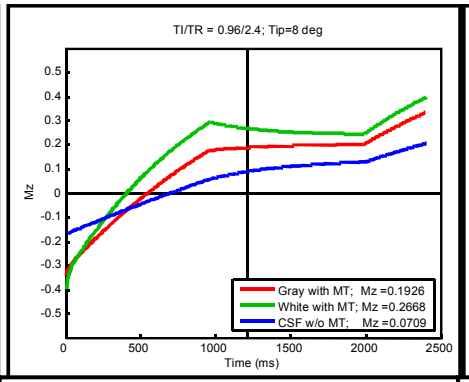

Fig. 25. 3D MPRAGE with conventional RF pulses and magnetization transfer.

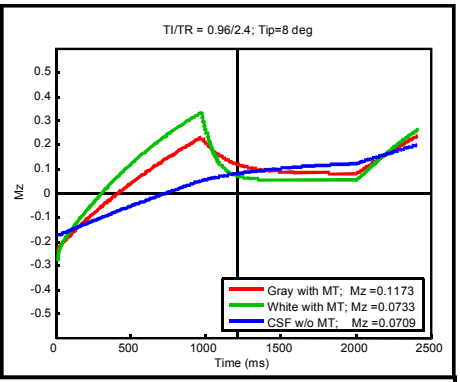

Fig. 26. 3D MPRAGE with B_1 insensitive pulses and magnetization transfer.

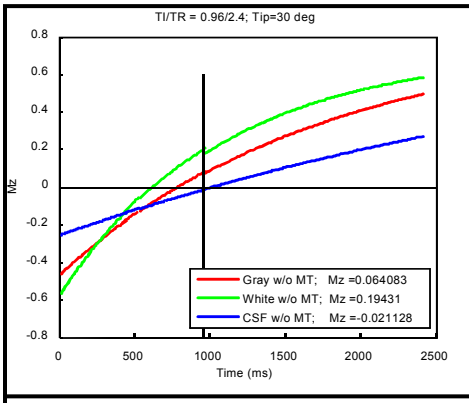

Fig. 27. 2D MPRAGE without magnetization transfer.

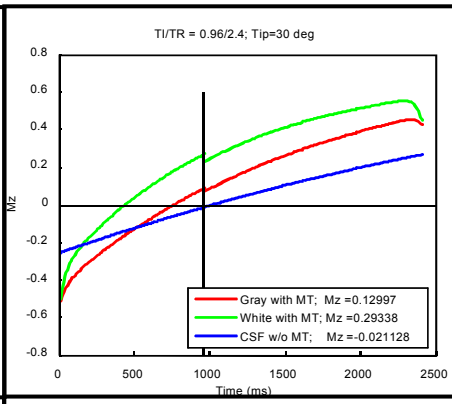

Fig. 28. 2D MPRAGE with conventional RF pulses and magnetization transfer.

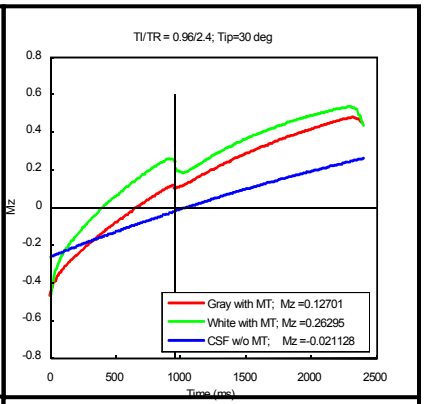

Fig. 29. 2D MPRAGE with B_1 insensitive pulses and MT.

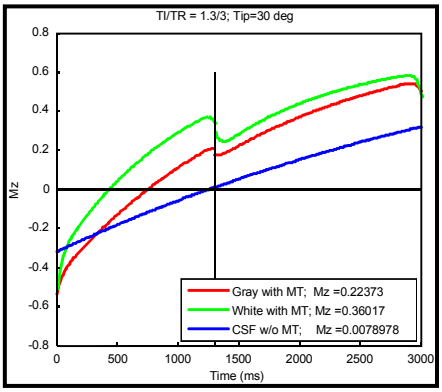

Fig. 30. 2D MPRAGE with B_1 insensitive RF pulses, MT, and longer TI and TR.

D. RESEARCH DESIGN AND METHODS

D.1. Overview: The research plan includes development of B_1 insensitive pulses, and lowered voltage spin echo pulses, as described below. **In addition, the research plan includes expansion of existing computer simulation experiments of MRI experiments, with inclusion of magnetization transfer (MT) effects.** Achievement of the aims of this project will facilitate improved acquisitions of structural, perfusion, diffusion, and susceptibility-weighted MRI, and support development of new methods providing improved signal, contrast to noise, and resolution as well as sensitivity for specific applications to support the research projects and clinical applications of the Resource Center. This project will also benefit a large number of funded ongoing collaborative and clinical research studies. Finally, in collaboration with other CIND scientists, incorporation of the best pulses into suitable MRI experiments, including relaxation and **perfusion** experiments, is planned.

D.2. MRI Instrument Time: The emphasis in this application is on the development of RF pulses, with proof of performance initially done through simulations. However, we will also work closely with other scientists within the Center for Imaging of Neurodegenerative Diseases (CIND) to simulate and re-design MRI sequences in order to implement pulses of interest into MRI experiments for the Bruker MedSpec 4.0 Tesla instrument (See below). In addition, there are a number of circumstances in which we expect to perform MRI experiments on normal individuals. For example, we will perform experiments to examine the B_1 strength and inhomogeneity over human heads covering a range of head sizes. In addition, we expect to perform initial MRI experiments to verify simulation results, and to assess SAR due to developed pulses. We estimate 4 hours of instrument/month for MRI experiments, which, as they come under the heading of development, are not charged.

D.3. Pulses with Immunity to B_1 Inhomogeneity (+/- 20% to 25%) (24 months)**:** The new B_1-insensitive design is based on optimized concatenations of rectangular pulses applied along different axes in the rotating frame, where the optimization is for both uniform tip and immunity to resonance offset. **As shown in the Preliminary Results section, the rectangular pulses may include off-resonance pulses to improve the tipping efficiency of the cascade.** The design focuses on excitation pulses, but includes extension of the method to spin echo and inversion pulses.

Special concatenated rectangular pulse sequences (excitation, inversion, and spin echo) with immunity to B_1 inhomogeneity and to resonance offset will be developed, but with the emphasis on excitation pulses. As shown in the Preliminary Results section, the concatenated sequences will be based on rectangular pulse concatenations in which the phases, off resonance conditions, and tip angles have been optimized for both immunity to B_1 inhomogeneity and to resonance offset. An example of the code for optimization of on-resonance rectangular pulse sequences (Written in Mathematica) is shown in Appendix B, and code for off-resonance pulses is shown in Appendix G. Even optimization of 3 pulse off-resonance sequences, and 4 pulse on-resonance sequences, proved difficult with a single processor computer without limiting the space of the search. While the Preliminary Results section showed results from a cascade of four pulses, we will make use of our multi-processor Beowulf computer (See Resources) to extend the optimization up to 6 pulses, and beyond if 6 pulses prove effective. However, our expectation is that the sequences will become overly long, and thus increasingly sensitive to resonance offset, at 6 pulses.

D.3.a. Rectangular Pulse Optimization: While no optimization algorithm is yet chosen for the Beowulf optimizations, a variety of open source optimization programs are available, including gradient and quasi-Newton methods (David-Fletcher-Powell and Broyden-Fletcher-Goldfarb-Shanno algorithms), as well as global optimization programs such as simulated annealing, and various stochastic methods (cluster methods). A large suite of optimization programs is available at www.netlib.org. Optimization methods will either limit the pulse angle of individual tips, or provide a penalty factor for larger individual tips. In addition, code requiring coalescence of resonance offsets will be developed for excitation pulses. While coalescence is not necessary for conventional MRI experiments, the coalescence does minimize T2* losses during the pulse and enables shorter TE times to be used.

D.3.b. Conversion of Rectangular Pulse Concatenation to Slice Selective Pulses: Conversion of on-resonance rectangular pulse cascades to slice select pulses is straightforward, although it does require

adjustment of gradient lengths when adjacent pulse tip angles are significantly different (different slice-selective tips require slightly different re-focusing gradients).

D.3.c. Slice-Selective Pulse Optimization: The PI's initial experience with slice selective pulses developed from concatenated sequences of rectangular pulses has been that the slice selective version may have either less or (surprisingly) more immunity to B_1 inhomogeneity than the rectangular pulse version. Thus, the optimal rectangular pulse sequence is not necessarily the optimal basis for the frequency selective version. Because of this, the initial slice selective version is regarded as a starting point, and further optimization will be done to try to further improve the pulse. The parameters to be optimized include:

1. The phase of each pulse
2. The tip angle of each pulse
3. The gradient length of each step

Optimization of the gradient refocusing lobe will be included as well.

In addition, we will look into including a cost function for overall pulse length and total rotation. The performance of the pulse will be assessed by integration of several measures. First, the magnitude profile will be examined over the slice (excluding transition zones) for correct tip angle. Second, the efficiency of the pulse will be assessed by integration of the signal over the slice width (including transition zones). Note that the signal is the square root of the sum of squares of the integration of the real and imaginary profiles, following correct gradient refocusing of the spins. Third, the contamination level will be assessed by integration of the magnitude profile outside of the slice. These measures will be taken over a range of B_1 field strengths and resonance offsets. Optimization will be done on the Beowulf computer. Although this latter optimization appears formidable, the parameters for the optimal slice selective pulse are not apt to be far from the starting point, so optimization over a fairly small range is contemplated. Furthermore, it is possible that further optimization does not bring significant improvement; if not, we will discontinue this latter optimization.

The aim will be to develop the following pulses, with emphasis on the first three categories, as adiabatic inversion and spin echo pulses already exist, albeit they are SAR intensive:

i) 90º excitation: The four pulse sequence of Figs. 5-8 will be our initial standard, and subsequent designs compared to it.

ii) Shallow tip excitation: The four pulse sequence of Figs. 9-11 generates considerable SAR (due to the large total rotation) for a shallow tip pulse. Other rectangular pulse optimized sequences with less total rotation (not shown) with nearly the performance of this pulse were obtained, but slice selective versions of these pulses have not yet been generated and tested.

iii) Excite pulses with intermediate tip angles: We were not as successful with generation of intermediate tip angle rectangular pulse sequences as with shallow and large tip angle pulses, although only designs of up to four pulses were explored. Thus, this area needs further exploration and development.

iv) Inversion pulses: The optimization code generated in Mathematica is valid for inversion pulses as well. In addition, we note that dual inversion pulses with proper phase inversion can perform as a double spin echo pulse, for observation of every second echo.

v) Spin echo pulses: While prelimlinary SE pulses with immunity have been developed (results not shown), further development and assessment of the feasibility of generating SE pulses with immunity to B_1 inhomogeneity will be done.

The importance of useable excitation pulses with immunity to B_1 over a range of at least +/- 20% justifies expenditure of considerable effort for further development of these pulses. In addition, inversion, and SE pulses with less total rotation than their adiabatic counterparts would constitute a very significant contribution.

D.4. Lower Peak Voltage Pulses (6 months)**:** The new, lowered peak voltage design method consists of concatenation of conventional, frequency-selective pulses with gradients of alternating sign. The design includes spoiler gradients incorporated into the spin echo pulse to shorten the overall length of the pulse. Operation of these pulses in inhomogeneous B_1 fields is also considered.

Lowered peak voltage spin echo (SE) (incorporating the crusher gradient into the pulse) and inversion (Inv) pulses will be designed through concatenation as discussed in the Preliminary Results section. The concatenation method with incorporation of crusher gradients represents an innovative design approach. The concatenated designs, like the conventional SLR pulses, are readily re-scaled for excitation of other frequency widths. Table 1 indicates the concatenated pulses to be developed. Resonance offsets, relaxation effects, and flow effects for execution of these pulses in a gradient of 20 mT/m (giving a nominal slice width of 4 mm) and 40 mT/m (nominal slice width of 2 mm) will be provided. To be most effective, dual spin echo pulses with reversed phases as shown in the Preliminary Results section are necessary to avoid losses due to B_1 inhomogeneity and resonance offset. Finally, the use of concatenation methods for reduced voltage excite and saturation pulses, and the use of quadratic-phase pulses [61] for saturation and inversion, and for reduced voltage dual spin echo pulses, will be further explored.

Table 1. Concatenated pulses

Pulse Phase	Pulse Type	Seg-ments	Tip	Width (kHz)	Effective Quality	Grad. Refocus	Reson. Offset	B_1	T1, T2	Flow
Linear	SE/Inv	3	180	3.2	4	☒	☒	☒	☒	☒
Linear	SE/Inv	3	180	3.2	8	☒	☒	☒	☒	☒

D.5. Implementation of Pulses into MRI Sequences (16 months)**:**

D.5.a. SAR Considerations for B_1 Insensitive Pulses: In all cases, replacing the original RF pulses with B_1 insensitive pulses increases the SAR of the experiment. For experiments producing low SAR, it should be possible to re-design the experiment to run with the B_1 insensitive pulses in approximately the original examination time, with the same S/N, but with improved fidelity (without the spatially varying contrast). In some cases, a re-designed experiment with longer repetition time, improved S/N, and a higher acceleration factor may be the ingredients to achieve the improved fidelity with similar examination time, while still staying within SAR limitations. However, for experiments that are already close to SAR limits, such as turbo spin echo experiments, improved fidelity can come only at the expense of a longer examination time. To better illustrate the trade-offs under consideration, SAR considerations for the 3D MP RAGE experiment are outlined below.

The literature suggests 1 kW of power applied to a headcoil should produce a B_1 field of 1 kHz[3,62]. This should be a conservative number, as it neglects any power absorbed by the coil itself. Assuming Kangarlu et al.'s suggestion that the weight of the human head makes up 5% of body weight[63], and using a weight of 90 kg, gives a head weight of 4.5 kg. The FDA SAR limit is 3.2 watts/kg, or, for this example, approximately 14 watts. Finally, let us assume a worst case example for producing a shallow tip angle using the B_1 immune on-resonance rectangular pulse sequence which requires 4 x 90^0, or 360 degrees of total rotation (Fig. 9). That is, with 1 kW of power the excitation pulse duration is 1 ms. The maximum number of these excitation pulses per second (to not exceed 3.2 watts/kg) is then 14. **Measurements of RF power presented at the 2007 RR Site Visit showed that the above calculations are entirely reasonable.**

The Bruker MedSpec 3D MPRAGE used by CIND scientists collects 120 lines of k space in 2.3 seconds, or 52 pulses/sec (neglecting the inversion pulse which occurs once every 2.3 seconds, and thus contributes very little to the SAR). Use of the newly designed off-resonance excitation pulses with an overall length of 1 ms lowers the wattage by a factor of 2, which still only allows 28 pulses/second. Lengthening the on resonance B_1 immune excitation pulse to 2 ms lowers the power by a factor of 4, and allows approximately 56 pulses/sec. However, this also lowers the immunity of the pulse to resonance offset. More importantly, replacing the original 100 us excitation pulse length with a 2 ms pulse length significantly lengthens the time of the experiment, and would require re-adjustment of the inversion time.

We have recently shown, by simulations of the 3D MPRAGE experiment, that lengthening the TR time by a factor of 2, and suitably re-adjusting the inversion time and excitation angle, can produce a S/N increase of approximately 2 (Preliminary Results). In principle, this would enable an acceleration factor of 4 to be used to reduce the examination time. However, as the MPRAGE experiment already uses an acceleration factor of 2, a more prudent approach would be to lengthen the TR time by just over 2 1/2 (giving an increased S/N by

approximately the same factor), so the experiment would require only 36 excitation pulses/sec, and use a total acceleration factor of 4 to keep the examination time close to the original time.

This brief example illustrates how a low SAR experiment can be re-designed to incorporate the more SAR intensive pulses into the experiment to produce the same S/N but with improved fidelity in essentially the same examination time. Moreover, we expect that simulation of other experiments will similarly reveal a broad range of parameters producing varying amounts of SAR, that can be used in conjunction with altered acceleration factors to achieve similar S/N and contrast in a similar examination time. However, for experiments already close to the SAR limit, the price for improved fidelity by incorporation of B_1 insensitive pulses will necessarily be lengthened examination time even with experiment re-design. Finally, details of any re-design depend on the pulses to be implemented, and on the amount of SAR reported by the MRI instrument.

D.5.b. Lowered Voltage Spin Echo Pulses: In contrast to the B_1 insensitive pulses, it should be possible to incorporate the lowered voltage spin echo pulses into existing experiments, with a concomitant increase in slice selective gradient, without significantly increasing the SAR of the experiment. In some case we will make use of CP phase cycling to improve the fidelity of every second echo as discussed in the Preliminary Results section of this proposal.

D.5.b.i. 1 T1-Weighted MRI: Although the primary emphasis of the pulse development section of this proposal is on the development of improved slice selective pulses for multislice MRI at high field, the PI will also work with other members of the CIND to implement these pulses into MRI sequences. The primary T1-weighted structural MRI being used by the CIND at 4.0 Tesla is a 3D MPRAGE sequence, which does not use slice selective pulses. Although the shallow tip rectangular pulse sequences shown in the Preliminary Results section could be implemented into a re-designed version of this experiment, our present thinking is that, due to the large total rotation (rotation an on-resonance spin would experience), the magnetization transfer effects would degrade the experiment **as indicated in the Preliminary Results section**. Instead, we will aim to generate a slice-selective (2D), whole brain sequence that can obtain results with similar S/N, hopefully in a similar examination time, as the original experiment, albeit with improved fidelity due the incorporation of the B_1 insensitive pulses. However, some lengthening of the examination time may be required to avoid exceeding the SAR limitations. The new experiment should largely negate the effects of non-uniform tipping, and significantly improve the ability to segment these images.

D.5.b.ii. T2-Weighted MRI: For the T2 weighted sequences, use will be made of excitation pulses with immunity to B_1 inhomogeneity, and for the SE pulses, we will implement the use of dual pulses with reversed phases (as discussed in the Preliminary Results section) to avoid the signal losses that would otherwise result from B_1 inhomogeneity and resonance offsets. It is anticipated that 2mm slice thickness will be used by CIND for the 4.0 Tesla T2-weighted structural MRI sequences. Some sacrifices may have to be made in terms of longer repetition time, to avoid exceeding SAR limits.

As the Bruker MedSpec turbo spin echo (TSE) sequences use an initial "stabilization" sequence, it is possible that the sequence could be improved by using B_1-insensitsive pulses for the stabilization section, and use normal pulses throughout the remainder of the sequence. Such an approach might lessen the effect of the B_1 inhomogeneity, while only slightly increasing the SAR of the sequence. This intriguing possibility will be explored through the simulations proposed (See below).

The PI will assist in additional implementation of pulses developed in this proposal into MRI sequences as appropriate.

D.5.b.iii. Relaxation Experiments: While a variety of MRI experiments for measurement of T1 in tissue are in use, most commonly used experiments can be divided into one of two categories: The first category consists of experiments using a number of time points, and for the most part are derived from the Look-Locker T1 experiment and implemented with a low angle FLASH experiment[64]. The second category makes use of only a very few time points, and are generally based on inversion recovery or saturation experiments (e.g., steady-state saturation under varied flip angles[65]). All of these experiments benefit from knowledge of the pulse angel(s) used in the experiment for improved accuracy of the calculated relaxation times. In addition, these experiments are not generally SAR intensive. Thus, we will implement B_1-insensitive pulses into T1 relaxation experiments in use by CIND scientists.

MRI experiments for measurement of T2 are invariably spin echo experiments, and accurate spin echo pulses are a necessity for measurement of accurate T2 values. Thus, we plan to implement B_1-insensitive pulses into T2 measurement sequences. Options include using B_1-insensitive pulses that we have developed, or using the lowered voltage spin echo pulses we have developed with CP phase cycling and using only every second echo for T2 measurements.

Further Development of MRI Simulation Programs (14 months): The simulation programs demonstrated for MP RAGE in the Preliminary Results section were written in Matlab with a user friendly, GUI interface (Appendix E), and include magnetization transfer (MT) effects (Appendix F). A further feature of these simulations is the ability to optimize the tip angles to maintain a constant signal intensity throughout a k-space traverse, with a prescribed roll-off of signal intensity at the edge of k-space. As the optimized tips depend on relaxation times[27], the optimization is for a particular tissue. However, averages of optimized tips for gray and white matter can be used to generate nearly flat responses for both of these tissues in the MP RAGE sequence. An example of these simulations for the 3D MP RAGE experiment is provided in Project 1 of the Acquisition Core.

These types of simulations will be expanded to other types of MRI experiments, including GRASE [66] experiments. In addition, Extended Phase Graph algorithms[28,29] will be used to simulate Turbo Spin Echo (TSE)[67] and MP SAGE[27] types of experiments. The simulations will include both magnetization transfer effects and the sensitivity of the experiment to off resonance effects, as well as providing for the calculation of optimized tips for flat signal responses.

While the primary purpose of these simulations is to quantify MT effects, they will also enable B_1 inhomogeneity effects to be examined, and will enable such strategies as the use of B_1 insensitive pulses for just the stabilization section of TSE (and other) sequences to assessed. A further, important use of these MRI simulations is expected to be in optimization of MRI sequences at 4.0 Tesla, taking into account advances provided by the reconstruction section of this grant for increased acceleration factors for MRI experiments.

D.6. Interactions

D.6.a. Interactions with other TRD projects: To the extent that implementation of improved RF pulses can improve the MRI sequences in use, this project will impact all other projects. In addition, the MRI computer simulations are also expected to provide improvement to some of the MRI sequences in use. In particular, this project will have strong interactions with Dr. Schuff's project (Acquisition Core 1) in providing improved RF pulses for T1 measurements, and the MRI simulations should enable optimization of acquisition parameters for FLASH and MP RAGE experiments, including calculation of variable flip angles. As the GRACE experiments being developed by Dr. Feinberg (Acquisition Core 2) can be thought of as turbo spin echo experiments with added gradient echo acquisitions, the improved RF pulses should also benefit these experiments, and this project will have strong interactions with Dr. Feinberg's project.

This project will also have interactions with the reconstruction core. First, the use of B_1 insensitive pulses is expected to enable more accurate image intensity normalization (and thus segmentation) to be performed. Second, the MRI data may be improved by optimization of acquisition parameters through the MRI simulations. Finally, this project will interact with the processing core, primarily through the MRI simulations. As the processing core enables sparser sampling and/or higher acceleration factors to be used, the simulations are expected to be invaluable in making optimal use of these improvements.

D.6.b. Interactions with collaborative projects: The combination of improved RF pulses and MRI simulations have the potential for improving imaging experiments used by all of the collaborative cores. This core is expected to have particularly strong interactions with Dr. Laxer's epilepsy core due to his emphasis on perfusion studies, which are expected to benefit from the B_1 insensitive pulses. However, interactions with the other collaborative projects, including will also be developed

E. HUMAN SUBJECTS RESEARCH

E.1. Protection of Human Subjects: A "protection of human subject" section has been written for the entire application in the main introduction section

F. VERTEBRATE ANIMAL: N/A

G. SELECT AGENT RESEARCH: N/A

H. LITERATURE CITED:

1. Hoult DI. Sensitivity and Power Deposition in a High-Field Imaging Experiment. J Magn Reson Imaging 2000;12:46-67.
2. Collins CM, Smith MB, Vaughan JT, Garwood M, Ugurbil K. B1 Field Homogeneity Comparison at 300 MHz: Calculation vs. Experiment. Proc Intl Soc Magn Reson Med 1999;7.
3. Vaughan JT, Garwood M, Collins CM, Liu W, DelaBarre L, Adriany G, Andersen P, Merkle H, Goebel R, Smith MB, Ugurbil K. 7T vs. 4T: RF power, homogeneity, and signal-to-noise comparison in head images. Magn Reson Med 2001;46(1):24-30.
4. Brinkmann BH, Manduca A, Robb RA. Optimized homomorphic unsharp masking for MR grayscale inhomogeneity correction. IEEE Trans Med Imaging 1998;17(2):161-171.
5. Han C, Hatsukami TS, Yuan C. A multi-scale method for automatic correction of intensity non-uniformity in MR images. J Magn Reson Imaging 2001;13(3):428-436.
6. Arnold JB, Liow JS, Schaper KA, Stern JJ, Sled JG, Shattuck DW, Worth AJ, Cohen MS, Leahy RM, Mazziotta JC, Rottenberg DA. Qualitative and quantitative evaluation of six algorithms for correcting intensity nonuniformity effects. Neuroimage 2001;13(5):931-943.
7. Cohen MS, DuBois RM, Zeineh MM. Rapid and effective correction of RF inhomogeneity for high field magnetic resonance imaging. Hum Brain Mapp 2000;10(4):204-211.
8. Sled JG, Zijdenbos AP, Evans AC. A nonparametric method for automatic correction of intensity nonuniformity in MRI data. IEEE Trans Med Imaging 1998;17(1):87-97.
9. Likar B, Maintz JB, Viergever MA, Pernus F. Retrospective shading correction based on entropy minimization. J Microsc 2000;197 (Pt 3):285-295.
10. Styner M, Brechbuhler C, Szekely G, Gerig G. Parametric estimate of intensity inhomogeneities applied to MRI. IEEE Trans Med Imaging 2000;19(3):153-165.
11. Vokurka EA, Thacker NA, Jackson A. A fast model independent method for automatic correction of intensity nonuniformity in MRI data. J Magn Reson Imaging 1999;10(4):550-562.
12. de Graaf RA, Nicolay K, Garwood M. Single-shot, B1-insensitive slice selection with a gradient-modulated adiabatic pulse, BISS-8. MagnResonMed 1996;35(5):652-657.
13. Hsu EW, Reeder SB, MacFall JR. Single-shot, variable flip-angle slice-selective excitation with four gradient-modulated adiabatic half-passage segments. Magn Reson Med 1998;40(2):334-340.
14. Saekho S, Yip CY, Noll DC, Boada FE, Stenger VA. Fast-kz three-dimensional tailored radiofrequency pulse for reduced B1 inhomogeneity. Magn Reson Med 2006;55(4):719-724.
15. Katscher U, Bornert P, Leussler C, van den Brink JS. Transmit SENSE. Magn Reson Med 2003;49(1):144-150.
16. Zhu Y. Parallel excitation with an array of transmit coils. Magn Reson Med 2004;51(4):775-784.
17. Silver MS, Joseph RI, Hoult DI. Highly selective pi/2 and pi pulse generation. JMagnReson 1984;59:347-351.
18. Conolly S, Glover G, Nishimura D, Macovski A. A reduced power selective adiabatic spin-echo pulse sequence. MagnResonMed 1991;18:28-38.
19. Tyszka JM, Mamelak AN. Quantification of B0 homogeneity variation with head pitch by registered three-dimensional field mapping. J Magn Reson 2002;159(2):213-218.
20. Wilson J, Jenkinson M, Jezzard P. Optimization of static field homogeneity in human brain using diamagnetic passive shims. Magn Reson Med 2002;48(5):906-914.
21. Wilson J, Jezzard P. Utilization of an intra-oral diamagnetic passive shim in fuctional MRI of the inferior frontal cortex. MagnResonMed 2003;50:1089-1094.
22. Cusack R, Russell B, Cox SM, De Panfilis C, Schwarzbauer C, Ansorge R. An evaluation of the use of passive shimming to improve frontal sensitivity in fMRI. Neuroimage 2005;24(1):82-91.
23. Matson GB. An integrated program for amplitude-modulated RF pulse generation and re-mapping with shaped gradients. MagnResonImaging 1994;12(8):1205-1225.

24. Conolly S, Nishimura D, Macovski A, Glover G. Variable-rate selective excitation. JMagnReson 1988;78:440-458.
25. Hennig J, Weigel M, Scheffler K. Calculation of flip angles for echo trains with predefined amplitudes with the extended phase graph (EPG)-algorithm: principles and applications to hyperecho and TRAPS sequences. Magn Reson Med 2004;51(1):68-80.
26. Busse RF. Reduced RF power without blurring: correcting for modulation of refocusing flip angle in FSE sequences. Magn Reson Med 2004;51(5):1031-1037.
27. Stocker T, Shah NJ. MP-SAGE: A new MP-RAGE sequence with enhanced SNR and CNR for brain imaging utilizing square-spiral phase encoding and variable flip angles. Magn Reson Med 2006;56(4):824-834.
28. Hennig J. Echoes- How to generate, recognize, use or avoid them in MR-imaging Sequences Part I: Fundamental and Not So Fundamental Properties of Spin Echoes. Concepts MagnReson 1991;3:125-143.
29. Scheffler K. A Pictorial Description of Steady-States in Rapid Magnetic Resonance Imaging. Concepts MagnReson 1999;11(5):291-304.
30. Hennig J, Scheffler K. Easy improvement of signal-to-noise in RARE-sequences with low refocusing flip angles. Rapid acquisition with relaxation enhancement. Magn Reson Med 2000;44(6):983-985.
31. Weigel M, Zaitsev M, Hennig J. Inversion recovery prepared turbo spin echo sequences with reduced SAR using smooth transitions between pseudo steady states. Magn Reson Med 2007;57(3):631-637.
32. Conolly S, Nishimura D, Macovski A. Variable-rate selective excitation for SAR reduction. Society of Magnetic Resonance in Medicine 1987.
33. Matson GB. Frequency selective RF pulses for multi-slice MRI with modest immunity to B1 inhomogeneity. 2001 2001. p 913.
34. Matson GB, Schleich T. Design of Null Pulses for use in Pulsed Arterial Spin Labeling by the Principle of Time Reversal. 2001. p 687.
35. Matson GB, Hill TC, Govindaraju V. Development of High Field Proton Spectroscopic Imaging for the Mouse Brain. 2001. p 1034.
36. Haxo RS. Computer Optimization of Selective Radiofrequency Pulses for Nuclear Magnetic Resonance, Magnetic Resonance Spectroscopy and Magnetic Resonance Imaging [Dissertation for Doctor of Philosophy in Chemistry]. Santa Cruz: University of California, Santa Cruz; 1990. 166 p.
37. Murdoch JB, Lent AH, Kritzer MR. Computer-optimized narrowband pulses for multislice imaging. JMagnReson 1987;74:226-263.
38. Garwood M, Ke Y. Symmetric pulses to induce arbitrary flip angles with compensation for RF inhomogeneity and resonance offsets. JMagnReson 1991;94:511-525.
39. Noll DC. A Genetic Algorithm for Optimal Design of Spectrally Selective k-Space. 2001. p 681.
40. Morrell G, Macovski A. Three-dimensional spectral-spatial excitation. MagnResonMed 1997;37:378-386.
41. Meyer CH, Pauly JM, Macovski A, Nishimura D. Simultaneous spatial and spectral selective excitation. MagnResonMed 1990;15:287-304.
42. Pauly JM, Hu BS, Wang SJ, Nishimura DG, Macovski A. A three-dimensional spin-echo or inversion pulse. MagnResonMed 1993;29:2-6.
43. Spielman D, Pauly J, Macovski A, Enzmann D. Spectroscopic imaging with multidimensional pulses for excitation: Simple. MagnResonMed 1991;19:67-84.
44. Star-Lack JM, Adalsteinsson E, Gold GE, Ikeda DM, Spielman DM. Motion correction and lipid suppression for /sup 1/H magnetic resonance spectroscopy. MagnResonMed 2000;43(3):325-330.
45. Stenger VA, Boada FE, Noll DC. Multi-Shot Three-Dimensional Tailored RF Slice-Select Pulses. 2001. p 347.
46. Stenger VA, Boada FE, Noll DC. Three-dimensional tailored RF pulses for the reduction of susceptibility artifacts in T(*)(2)-weighted functional MRI. Magn Reson Med 2000;44(4):525-531.
47. Levitt MH. Symmetrical composite pulse sequences for NMR population inversion. I. Compensation of radiofrequency field inhomogeneity. JMagnReson 1982;48:234-264.
48. Shen J. Composite slice-selective 90 degree excitation pulses with adiabaticity. Proc Intl Soc Mag Reson Med 2002;10:2498.

49. Thesen S, Kruger G, Mueller E. Compensation of dielectric resonance effects by means of composite excitation pulses. Proc Intl Soc Mag Reson Med 2003;11:715.
50. Chen Y, Young K, Schleich T, Matson GB. Frequency selective RF pulses for multislice MRI with modest immunity ti B1 inhomogeneity and to resonance offset. Proc Intl Soc Mag Reson Med 2004;11:2652.
51. Golay X, Stuber M, Pruessmann KP, Meier D, Boesiger P. Transfer insensitive labeling technique (TILT): application to multislice functional perfusion imaging. JMagnResonImaging 1999;9(3):454-461.
52. Pruessmann KP, Golay X, Stuber M, Scheidegger MB, Boesiger P. RF pulse concatenation for spatially selective inversion. JMagnReson 2000;V146(N1):58-65.
53. Pauly J, Le Roux P, Nishimura D, Macovski A. Parameter relations for the Shinnar-Le Roux selective excitation pulse design algorithm. IEEE TransMedImaging 1991;10:53-65.
54. Helms G, Hagberg GE. Pulsed Saturation of the Standard Two-Pool Model for Magnetization Transfer. Part I: The Steady State. Concepts MagnReson 2004;21A(1):37-49.
55. Deichmann R, Good CD, Josephs O, Ashburner J, Turner R. Optimization of 3-D MP-RAGE sequences for structural brain imaging. Neuroimage 2000;12(1):112-127.
56. Li JG, Graham SJ, Henkelman RM. A flexible magnetization transfer line shape derived from tissue experimental data. Magn Reson Med 1997;37(6):866-871.
57. Stanisz GJ, Odrobina EE, Pun J, Escaravage M, Graham SJ, Bronskill MJ, Henkelman RM. T1, T2 relaxation and magnetization transfer in tissue at 3T. Magn Reson Med 2005;54(3):507-512.
58. Cercignani M, Symms MR, Ron M, Barker GJ. 3D MTR measurement: from 1.5 T to 3.0 T. Neuroimage 2006;31(1):181-186.
59. Ramani A, Dalton C, Miller DH, Tofts PS, Barker GJ. Precise estimate of fundamental in-vivo MT parameters in human brain in clinically feasible times. Magn Reson Imaging 2002;20(10):721-731.
60. Johnson G, Wadghiri YZ, Turnbull DH. 2D multislice and 3D MRI sequences are often equally sensitive. Magn Reson Med 1999;41(4):824-828.
61. Schulte RF, Tsao J, Boesiger P, Pruessmann KP. Equi-ripple design of quadratic-phase RF pulses. J Magn Reson 2004;166(1):111-122.
62. Vaughan JT, Hetherington HP, Otu JO, Pan JW, Pohost GM. High frequency volume coils for clinical NMR imaging and spectroscopy. MagnResonMed 1994;32(2):206-218.
63. Kangarlu A, Ibrahim TS, Shellock FG. Effects of coil dimensions and field polarization on RF heating inside a head phantom. Magn Reson Imaging 2005;23(1):53-60.
64. Haase A, Frahm J, Matthaei D, H„nicke W, Merboldt K-D. FLASH imaging. Rapid NMR imaging using low flip-angle pulses. JMagnReson 1986;67:258-266.
65. Cheng HL, Wright GA. Rapid high-resolution T(1) mapping by variable flip angles: accurate and precise measurements in the presence of radiofrequency field inhomogeneity. Magn Reson Med 2006;55(3):566-574.
66. Feinberg DA, Kiefer B, Johnson G. GRASE improves spatial resolution in single shot imaging. MagnResonMed 1995;vol.33,(no.4):529-533.
67. Hennig J. Multiecho Imaging Sequences with Low Refocusing Flip Angles. JMagnReson 1988;78:397-407.